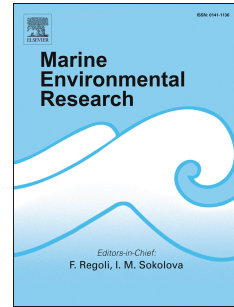


Journal Pre-proof

The impact of climate change on the geographical distribution of habitat-forming macroalgae in the Rías Baixas

M. Des, B. Martínez, M. deCastro, R.M. Viejo, M.C. Sousa, M. Gómez-Gesteira



PII: S0141-1136(20)30273-7

DOI: <https://doi.org/10.1016/j.marenvres.2020.105074>

Reference: MERE 105074

To appear in: *Marine Environmental Research*

Received Date: 20 March 2020

Revised Date: 25 June 2020

Accepted Date: 4 July 2020

Please cite this article as: Des, M., Martínez, B., deCastro, M., Viejo, R.M., Sousa, M.C., Gómez-Gesteira, M., The impact of climate change on the geographical distribution of habitat-forming macroalgae in the Rías Baixas, *Marine Environmental Research* (2020), doi: <https://doi.org/10.1016/j.marenvres.2020.105074>.

This is a PDF file of an article that has undergone enhancements after acceptance, such as the addition of a cover page and metadata, and formatting for readability, but it is not yet the definitive version of record. This version will undergo additional copyediting, typesetting and review before it is published in its final form, but we are providing this version to give early visibility of the article. Please note that, during the production process, errors may be discovered which could affect the content, and all legal disclaimers that apply to the journal pertain.

© 2020 Published by Elsevier Ltd.

Author Statement:

MD, BM, MdC, RMV and MGG conceived and designed the study. MD, MdC and MGG conducted the numerical simulations. BM and RMV conducted the fieldwork. MD, MdC and MGG analyzed the data. MD wrote the first draft of the manuscript. All authors contributed to the discussion and revision of the manuscript.

Journal Pre-proof

The impact of climate change on the geographical distribution of habitat-forming macroalgae in the Rías Baixas

M. Des^{a*}, B. Martínez^b, M. deCastro^a, R. M. Viejo^b, M.C. Sousa^c and M.
Gómez-Gesteira^a

^aEnvironmental Physics Laboratory (EphysLab), CIM-UVIGO, Universidade de Vigo, Edificio Campus da Auga, 32004 Ourense, Spain.

^bDepartamento de Biología y Geología, Universidad Rey Juan Carlos, E-28933, Móstoles, Madrid, Spain,

^cCESAM, Physics Department, University of Aveiro, Aveiro 3810-193, Portugal.

*Corresponding author.

E-mail address: mdes@uvigo.es (M. Des).

Abstract

In the current scenario of climate change characterized by a generalized warming, many species are facing local extinctions in areas with conditions near their thermal tolerance threshold. At present, the southern limit of the geographical distribution of several habitat-forming algae of cold-temperate affinities is located in the Northwest Iberian Peninsula, and the Rías Baixas may be acting as contemporary refugia at the range edge. Therefore, it is necessary to analyze future changes induced by ocean warming in this area that may induce changes in macroalgae populations. The Delft3D-Flow model forced with climatic data was used to calculate July-August sea surface temperature (SST) for the present (1999-2018) and for the far future (2080-2099). Mean daily SST was used to develop and calibrate a mechanistic geographical distribution model based on the thermal survival threshold of two intertidal habitat-forming macroalgae, namely *Himantalia elongata* (L.) S.F.Gray and *Bifurcaria bifurcata* R. Ross. Results show that *H. elongata* will become extinct in the Rías Baixas by the end of the century, while *B. bifurcata* will persist and may occupy potential free space left by the decline in *H. elongata*.

Keywords: climate change; macroalgae; intertidal organisms; mechanistic species distribution model; Delft3D;CORDEX; CMPI5; RCP8.5

28 1. Introduction

29 Ecological systems have to face the modification in environmental conditions
30 that global climate change is causing worldwide (Chen et al., 2011; McMenamin et al.,
31 2008; Parmesan et al., 1999; Poloczanska et al., 2013, 2016). In terrestrial and marine
32 environments, species have to deal with a general increase in warming conditions,
33 which is not spatially homogeneous (Cane et al., 1997). Often, warming results in local
34 extinctions at the low latitude range limits of the species distributions (Russell et al.,
35 2013; Wiens, 2016). Range contraction and local extinction or decrease are especially
36 worrying when affecting habitat-forming species that provide structure, shelter and food
37 to many accompanying species, behaving like ecosystem engineers (*sensu* Jones et al.,
38 1994). The pattern of climate change and, in particular, warming, may be heterogeneous
39 across the latitudinal gradient of a species distribution (Helmuth et al., 2006) and there
40 may be colder favorable spots at the range margins. These cold spots may act as
41 contemporary climatic refugia (Ashcroft, 2010; Keppel et al., 2012), favoring the
42 persistence of edge populations.

43 Bakun (1990) hypothesized that global warming could strengthen coastal
44 upwelling intensity due to the increase in land-ocean thermal contrast. The
45 strengthening of upwelling-favorable winds would result in cooling of the ocean
46 surface. This hypothesis has been tested for different upwelling systems, finding
47 different trends and concluding that each system responds to global warming differently
48 (Sydeman et al., 2014; Varela et al., 2015; Wang et al., 2015). On the other hand,
49 coastal upwelling regions show lower warming rates than the adjacent ocean (Santos et
50 al., 2012a, b; Bakun et al., 2015; Varela et al., 2018; Seabra et al., 2019). In the same
51 way, the areas affected by river plumes usually show lower warming rates than the

52 adjacent ocean water (Costoya et al., 2017, 2016). Thereby, coastal upwelling regions,
53 estuaries and adjacent coastal areas may represent climatic refugia for many species.

54 Coastal rocky systems are among the most productive marine areas (Smale and
55 Wernberg, 2013). In temperate latitudes, these environments are dominated by
56 macroalgae which are declining at a global scale (Kumagai et al., 2018). Kelp forests
57 and the large intertidal macroalgae meadows are threatened in many regions of the
58 planet by climate change, other anthropogenic stressors and local factors (Strain et al.,
59 2014; IPCC, 2015; Krumhansl et al., 2016; Wernberg et al., 2016). The geographical
60 distribution of these species has traditionally been related to water temperature, in
61 addition to other physical factors of regional and local variation, such as marine salinity
62 (reviewed in Lüning, 1990). The southern, lower latitudinal limit of the geographic
63 distribution of several kelps and large intertidal seaweeds is located in the Northwest
64 Iberian Peninsula (NWIP). A marked contraction of the species ranges in this area has
65 been detected in recent years (reviewed in Casado-Amezúa et al., 2019). This is the case
66 of *H. elongata*, which has disappeared from a coastal strip of approximately 130 km
67 since the start of this century in the North Iberian Peninsula (NIP) (Duarte et al., 2013),
68 feasibly due to its restricted thermal tolerance (Martínez et al., 2015). Currently, its
69 distribution is limited to the NWIP corner, including the presence inside the large
70 embayments of the Galician rias and in areas moderately exposed to waves (Martínez et
71 al., 2012). This species exemplifies the decline response observed in other habitat-
72 forming macroalgae of cold-temperate affinities. By contrast, the degree of resilience to
73 warming of other macroalgae with greater tolerance to thermal stress, such as *B.*
74 *bifurcata*, is still unknown. Currently, the southern limit of *B. bifurcata* is located
75 around upwelling south Morocco regions (Neiva et al., 2015). It helps to explain the *B.*
76 *bifurcata* shifted southwards in Portugal observed by Lima et al. (2007). Martínez et al.

77 (2012) projected an increase of its presence in NW Iberia using SST anomalies for the
78 near future (2040). Recent studies indicate that these species of warm-temperate affinity
79 are declining in NIP (Méndez-Sandín and Fernández, 2016). Moreover, models of the
80 whole geographical distribution projected a northward shift of its southern limit and its
81 expansion from its high latitude range limit to Scotland or even Norway (Neiva et al
82 2015).

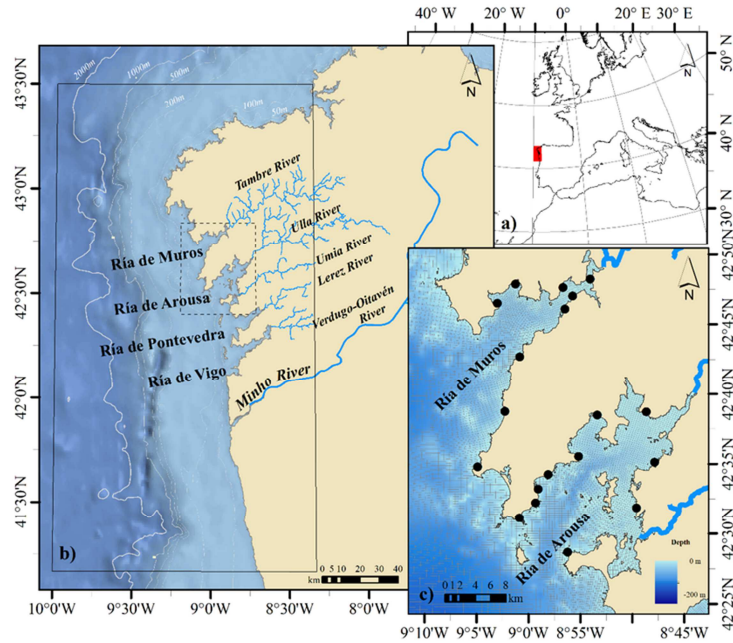
83 Additionally, changes in the distribution of seaweeds could also be related to
84 upwelling variations (Sánchez et al., 2005). The abundance and distribution of seaweeds
85 also depend on important environmental factors, such as exposure to waves and the
86 availability of hard substrate for attachment (Martínez et al., 2012), and anthropogenic
87 factors, as pollution (Fairweather, 1990). It should be noted, that pollution mitigation
88 policies, such as the EU Water Framework Directive (WFD) 2000/60/EC, promoted an
89 improvement in water quality that can lead to a partial recovery of seaweeds
90 communities (Díez et al., 2009, 2012).

91 The Rías Baixas are four flooded incised valleys (Evans and Prego, 2003)
92 located on the NWIP, at the northern limit of the eastern North Atlantic Upwelling
93 system. They are the southernmost rias of Galicia (Fig. 1). Due to their location, they
94 are strongly influenced by upwelling events. Upwelling, together with other co-varying
95 factors such as the higher water nutrient supply, protection from wave action or river
96 flow (Duarte and Viejo, 2018) may be responsible for the rias to be acting as
97 contemporary refugia to warming (Santos et al., 2011) for large, habitat-forming
98 macroalgae (Lourenço et al., 2016). Although it is expected an intensification of
99 upwelling-favorable winds in the NWIP for the future (Rykaczewski et al., 2015; Sousa
100 et al., 2017), Sousa et al. (2020) have recently shown that coastal upwelling will be less
101 effective due to the increase in the stratification of the upper layer caused by sea surface

102 warming. In fact, Des et al. (2020) determined that the future increase in water
103 temperature and stratification may negatively affect the growth of *Mytilus*
104 *galloprovincialis*, the most common species of mussel cultured in the area. Given this
105 previous research, a question immediately arises: will the Rías Baixas act as climatic
106 refugia against seawater warming for large habitat-forming macroalgae in the future?

107 The aim of this work is to determine how climate change, and SST warming in
108 particular, will affect the geographical distribution of two intertidal macroalgae, *H.*
109 *elongata* and *B. bifurcata*, within the Rías Baixas. These two species are large, canopy-
110 forming algae that dominate the low intertidal levels of the rocky shores of the eastern
111 Atlantic, which modify the environment and provide shelter and food for a wide variety
112 of organisms (e.g. Niell, 1981; Anadó, 1983; Fernández et al., 1983; Hawkins and
113 Hartnoll, 1985; Gestoso et al., 2010).

114 Firstly, SST data, computed by means of Delft3D-Flow numerical model, were
115 used to detect heat waves that may affect each of the species. Then, a mechanistic
116 distribution model based on the thermal survival threshold for adult plants of each
117 species was calibrated and used to determine the thermal habitat suitability for the
118 present (1999-2018) and by the end of the century (2080-2099). Thermal survival
119 thresholds for adult plants were previously determined by Martínez et al. (2015).



120
 121 **Fig. 1.** (a) Location of the study area along the northwestern coast of the Iberian Peninsula. (b) The box
 122 indicates the modeled area. (c) A close-up view of the Ria de Muros and the Ria de Arousa is shown with
 123 the numerical grid and the position of TidbiT data loggers sampling stations (black points).

124 2. Methodology

125 2.1. Hydrodynamic numerical model

126 Sea surface temperature (SST) was computed using the hydrodynamic numerical
 127 model Delft3D-Flow. Numerical simulations of transport conditions were performed
 128 using the mesh, parametrization and implementation previously validated for the Rías
 129 Baixas by Des et al. (2019, 2020). The main characteristics of the numerical model
 130 configuration are described below; however, for a more detailed description of the
 131 parametrization see Des et al. (2019, 2020).

132 The computational grid covers from 8.33°W to 10.00°W and from 41.18°N to
 133 43.50°N (Fig. 1b, rectangle). A curvilinear irregular grid was adopted with 452 x 446
 134 cells, and a mean resolution of 2200 m × 800 m on the west boundary, gradually
 135 increasing towards onshore, allowing higher resolution in the Rias (220 m x 140 m) and

136 the Minho estuary ($50 \text{ m} \times 77 \text{ m}$). This high spatial resolution allows Delft3D-Flow to
137 provide, among other variables, SST data in the areas of the Rías Baixas that represent
138 the natural habitats for intertidal macroalgae such as *H. elongata* and *B. bifurcata*. The
139 model uses 16 sigma layers with refined surface layers at the surface.

140 The bathymetric dataset for model simulations was created compiling data from
141 different sources. Multibeam-sourced bathymetry with a resolution of 5 m for the rias of
142 Vigo and Pontevedra was provided by the General Fishing Secretary. The bathymetry of
143 the Ría de Arousa, the Ría de Muros and the adjacent shelf area was obtained from
144 nautical charts of the Spanish Navy Hydrographical Institute. The Minho estuary
145 bathymetry was provided by the Portuguese Navy Hydrographic Institute. Gaps in the
146 dataset were filled using data from the General Bathymetric Chart of the Oceans with a
147 horizontal resolution of 30 arc seconds (GEBCO, <https://www.gebco.net/>).

148 The oceanic boundary was forced with transport conditions (salinity and water
149 temperature) and water level. Tidal harmonic constituents (M_2 , S_2 , N_2 , K_2 , K_1 , O_1 , P_1 ,
150 Q_1 , M_{sF} , MM , M_4 , MS_4 , MN_4) were obtained from the model TPXO 7.2
151 TOPEX/Poseidon Altimetry (<http://volkov.oce.orst.edu/tides/global.html>) and were
152 prescribed as astronomical forcing at the oceanic open boundary. River discharges are
153 imposed as fluvial open boundary condition. The exchange of heat through the free
154 surface was simulated using the “absolute flux, net solar radiation” model. This model
155 requires relative humidity, air temperature and the combined net solar (short wave) and
156 net atmospheric (longwave) radiation. The heat loss due to evaporation and convection
157 is computed by the model (Deltares, 2014). Wind components and pressure values are
158 imposed varying spatially.

159 Following the procedure described by Des et al. (2020), two numerical
160 experiments were performed. In the first one (Exp#1 from now on), Delft3D was mainly

161 forced with measured and reanalysis data, and the hydrodynamics of the study area was
162 simulated for a historical period. In the second experiment (Exp#2 from now on), the
163 model was mainly forced with historical and future data from the Regional Circulation
164 Models (RCM) driven by General Circulation Models (GCM) executed in the
165 framework of the Coordinated Regional Climate Downscaling Experiment (CORDEX)
166 project (<http://www.cordex.org/>). Both experiments were run for July and August using
167 a spin-up period of two weeks.

168 Exp#1 was run for 2012 to be compared with *in situ* coastal temperature data.
169 The thermohaline boundary conditions for Exp#1 were imposed using daily data from
170 the operational Atlantic-Iberian Biscay Irish-Ocean Physics Reanalysis
171 (<http://marine.copernicus.eu/>). Data from MeteoGalicia Weather Research and
172 Forecasting Model (<https://www.meteogalicia.gal>), were used as surface boundary
173 conditions. Minho River discharge data were provided by the Confederación
174 Hidrográfica Miño-Sil (<http://saih.chminosil.es>), while Verdugo-Oitavén, Lerez, Ulla,
175 and Umia rivers discharge data were retrieved from the MeteoGalicia database.

176 Exp#2 was run for the historical (1999 - 2018) and future (2080-2099) periods
177 under climatic conditions to perform geographical distribution maps of *H. elongata* and
178 *B. bifurcata* for the present and the future climate periods. Data for ocean boundary
179 conditions were retrieved from the MOHC-HadGEM2-Es GCM outputs ([https://esgf-
180 node.ipsl.upmc.fr/projects/esgf-ipsl/](https://esgf-node.ipsl.upmc.fr/projects/esgf-ipsl/)). Surface boundary conditions were obtained from
181 the MOHC-HadGEM2-Es-RCA4 RCM outputs (<http://www.cordex.org/>). Among the
182 available scenarios, the RCP8.5 greenhouse gas emission scenario was considered for
183 future projections. This scenario is quite likely considering the current increase in
184 greenhouse gas emission (Brown and Caldeira, 2017). Climatologic river discharge data
185 were obtained from the Hype Web portal (<https://hypeweb.smhi.se>) and a reduction of

186 25% in river discharge was considered for future projections
 187 (<https://hypeweb.smhi.se/explore-water/climate-impacts/europe-climate-impacts/>).

188 2.1.1. Validation of the Hydrodynamic numerical model

189 As stated above, the capability of the hydrodynamic numerical model to
 190 reproduce the hydrodynamic conditions of the Rías Baixas was previously assessed and
 191 validated by Des et al. (2019, 2020). In addition, further checking of the skill of the
 192 numerical model to reproduce water temperature in shallow coastal areas was carried
 193 out using temperature data measured *in situ* using 19 TidbiT data loggers (9 located in
 194 the Ría de Muros and 10 in the Ría de Arousa, Fig. 1c). Data loggers recorded the
 195 temperature every 30 minutes from January 2012 to September 2013, but only
 196 temperatures of August 2012 at the time of high tides were used to validate the model.
 197 *In situ* water temperature measurements were compared with simulated temperature
 198 data using the root mean square error, bias and Pearson product-moment correlation.

199 The root mean square error (RMSE), bias and Pearson product-moment
 200 correlation (r) were calculated as

$$201 \quad RMSE = \left\{ \frac{1}{N} \sum_{i=1}^N |X_{obs}(t_i) - X_{mod}(t_i)|^2 \right\}^{1/2} \quad (1)$$

$$202 \quad Bias = \frac{1}{N} \sum_{i=1}^N (X_{mod}(t_i) - X_{obs}(t_i)) \quad (2)$$

$$203 \quad r = \frac{\sum_i (x_{obs}(t_i) - \bar{x}_{obs})(x_{mod}(t_i) - \bar{x}_{mod})}{\sqrt{\sum_i (x_{obs}(t_i) - \bar{x}_{obs})^2} \sqrt{\sum_i (x_{mod}(t_i) - \bar{x}_{mod})^2}} \quad (3)$$

204 where $X_{obs}(t_i)$ and $X_{mod}(t_i)$ are the observed (measured *in situ*) and modeled
 205 (computed—with Delft3D) water temperature, respectively, and N is the number of
 206 samples. Bias and RMSE were averaged in order to obtain a mean value for each
 207 station.

208 2.2. Mechanistic modeling of the geographic distribution of macroalgae

209 The distribution models were based on the thermal tolerance threshold for the
210 species survival. The water temperature data obtained from the first layer of the
211 hydrodynamic model was considered as the predictive variable because SST is
212 significantly correlated with the distribution of *H. elongata* and *B. bifurcata*, as it
213 happens, in general, for seaweeds (Lüning, 1990; Martínez et al., 2012). The number of
214 days (with a minimum number of 10 consecutive days) during which the daily mean
215 SST was higher than the physiological threshold of the algae was calculated for the
216 coastal areas of the Rías Baixas. For a better understanding, result were expressed as
217 percentage of time both for historical (July-August 1999 - 2018) and future (July-
218 August 2080-2099) periods. The physiological thresholds considered are based on the
219 lethal conditions determined by Martínez et al. (2015) using adult fronds in tank
220 experiments. This lethal conditions occurred when the mean seawater temperature
221 exceeded the specific threshold value of the species, 18 °C and 24.7 °C, for *H. elongata*
222 and *B. bifurcata*, respectively, sometime between days 6 and 13 of the experiment
223 (Martínez et al., 2015). To determine the exact value, the analysis based on the thermal
224 stress was carried out for different heat-wave durations ranging from 6 to 13, adopting
225 in the rest of the study the duration of extreme heat waves that provides the best score.

226 The presence/absence of *H. elongata* and *B. bifurcata* on the shore of the Rías
227 Baixas was determined from a field survey carried out in 2005 to model the distribution
228 of these species in the Atlantic Spanish coast (Martínez et al., 2012). A total of 81
229 locations were visited inside Rías Baixas. The locations in Muros and Arousa Rias were
230 revisited again in 2011 to verify if the distribution of algae had changed since 2005.
231 Substrate and wave action are, together with the thermal conditions, the main factors
232 influencing the settlement of *H. elongata* (Martínez et al. 2012). Therefore, those points

233 where the presence of *H. elongata* is less probable due to the existence of muddy and
234 sandy substrates were discarded from the analysis. This was determined using the
235 geological maps provided by the Spanish Geological and Mining Institute (IGME) and
236 the information from field campaigns. Additionally, those points where the presence of
237 *H. elongata* is less probable due to the significant wave height
238 (<https://www.meteogalicia.gal/modelos/>) were also discarded. The distributional records
239 of *H. elongata* were used to adjust the mechanistic distribution model. This species was
240 preferred over *B. bifurcata* because shows less prevalence in the study area. As the
241 presence of a stable population depends on the conditions of several years, the map of
242 percentage of time under lethal conditions for July-August 1999-2011 was used to
243 perform the calibration. A percentage of time of approximately 33% was identified as
244 the threshold for the presence of populations, i.e., none of the present populations was
245 found in grid cells with more than 33% of the days under lethal conditions, which are
246 the periods of at least 10 consecutive days of daily mean SST > 18 °C (see results). This
247 threshold was used to interpret the current (1999-2018) *H. elongata* maps of thermal
248 habitat suitability, and their future (2080-2099) projections. Areas where the time under
249 lethal conditions exceeds the 33% threshold were interpreted as locations of algae
250 absence. For the remaining areas, three levels of habitat thermal suitability were
251 defined: 1) P1 for values between 0 and 11% ([0, 11] %), representing the optimal
252 conditions, far from the lethal threshold, 2) P2 for intermediate values ((11, 22] %), and
253 3) P3 for values between 22 and 33% ((22, 33] %), that may represent sub-lethal
254 temperature conditions. The same criteria were used to interpret the *B. bifurcata*
255 distribution maps (using a thermal survival threshold of 24.7 °C, see results).

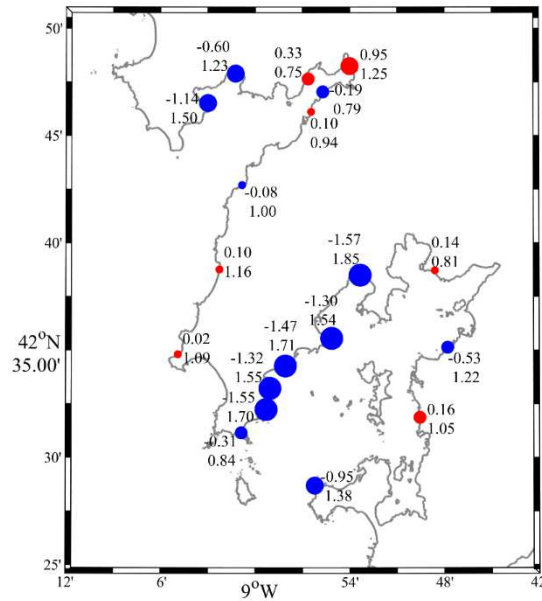
256 Favorability maps were made to indicate the likelihood of the presence of
257 suitable conditions for *H. elongata* and/or *B. bifurcata* by comparing the maps of

258 thermal habitat suitability. The high suitability values (lethal conditions < 33% of the
259 time) in a grid cell implies that *H. elongata* and *B. bifurcata* can be found. This fact was
260 indicated on the map as coexistence. When the suitability values indicate the absence of
261 *H. elongata*, but the presence *B. bifurcata*, this was labeled on the map as *B. bifurcata*.
262 Finally, when the suitability conditions in a grid cell are unfavorable for both algae, it
263 was indicated as none.

264 3. Results and discussion

265 3.1. SST validation

266 Modeled and *in situ* water temperature at 1 m depth for August 2012 were
267 compared by means of the mean bias and RMSE calculated for each TidbiT logger
268 station (Figure 2). The pattern observed is similar in both rias and, in general, the model
269 tends to underestimate *in situ* water temperature along the northern shores of the rias
270 (Fig. 2 blue dots, negative bias). The model tends to overestimate the water temperature
271 in the inner areas (Fig. 2 red dots, positive bias) and the bias is almost zero along the
272 southern shores. The maximum positive, 0.95 °C, and negative, -1.57 °C bias observed
273 are quite similar to those obtained by Des et al. (2020), 1.25 °C and -1.44 °C,
274 respectively. In general, there are more stations with high bias and RMSE than observed
275 in Des et al. (2019, 2020) where *in situ* vertical profiles are located in deeper areas.
276 These higher errors are likely due to both the location of the loggers in coastal intertidal
277 areas and the limited horizontal resolution of the mesh due to the complex orography of
278 the rias. Following a similar procedure to that developed in de Pablo et al., (2019), the
279 mean Pearson correlation coefficients were calculated for the Ría de Muros (0.82) and
280 for the Ría de Arousa (0.80). Both values show a good agreement between observations
281 and model results.



282

283

284

285

286

Fig. 2. Mean values of bias (upper number) (°C) and RMSE (lower number) (°C) obtained comparing Delft3D-Flow modeled and measured water temperature at 1 m depth for August 2012. Red dots indicate that the model overestimates *in situ* data (positive bias). Blue dots indicate that the model underestimates *in situ* data (negative bias). Dot size indicates the bias percentile.

287

3.2. Calibration of the species distribution model

288

289

290

291

292

293

294

295

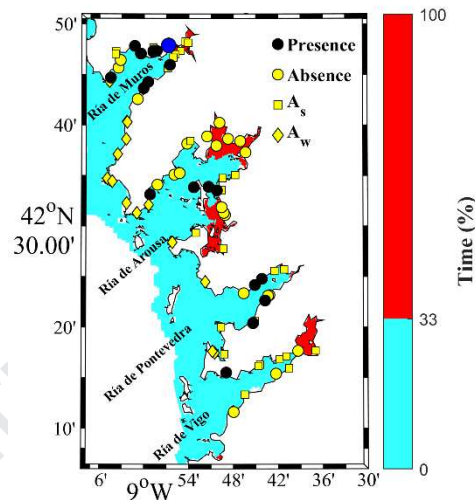
296

297

298

Based on the experiments developed in Martínez et al., (2015), where the lethal conditions for *H. elongata* occurred sometime between days 6 and 13 of the experiment, a thermal stress analysis was performed in which several heat-waves were considered with durations between 6 and 13 days. 10-day heat-wave was shown to provide the highest number of presence/absence successes regarding field data and it was considered for further analysis. Additionally, the maximum percentage of time under lethal conditions suffered by any stable population of *H. elongata* for the period 1999-2011 (July-August) was 33%. In this study, this value was observed for the northernmost population located in the inner part of the Ría de Muros (Fig. 3, blue dot). When applying this threshold, the mechanistic models properly classify 18 presences (100% of sensitivity) and 10 absences, providing 13 false presences (Fig. 3, filled

299 yellow dots located in the cyan area). This is well known limitation of mechanistic
 300 distribution models based only on the physiological threshold of the species, which tend
 301 to over-predict species prevalence (Martínez et al., 2015). The false presences can be
 302 associated to other environmental factors, such as high atmospheric temperatures during
 303 low tide affecting those individuals inhabiting the low intertidal, the tidal range or the
 304 wind speed (Martínez et al., 2012, de la Hoz et al., 2019). Despite the model tending to
 305 over-predict the presence of *H. elongata*, it can provide useful information about
 306 potential areas of extinction in the future.



307

308 **Fig. 3.** Percentage of time (July-August 1999-2011) during which *H. elongata* supports
 309 lethal conditions. Filled black points indicate the presences. Filled yellow points indicate the
 310 absences. Filled yellow squares indicate absences associated with unfavorable substrate or/and
 311 unfavorable significant wave height (Absence_{sw}). Data recorded in a field survey carried out in 2005
 312 (and re-surveyed in 2011). Filled blue point indicates the location of the presence record which
 313 tolerates lethal conditions for more percentage of time. Cyan represent areas suitable for presence
 314 and red for absence.

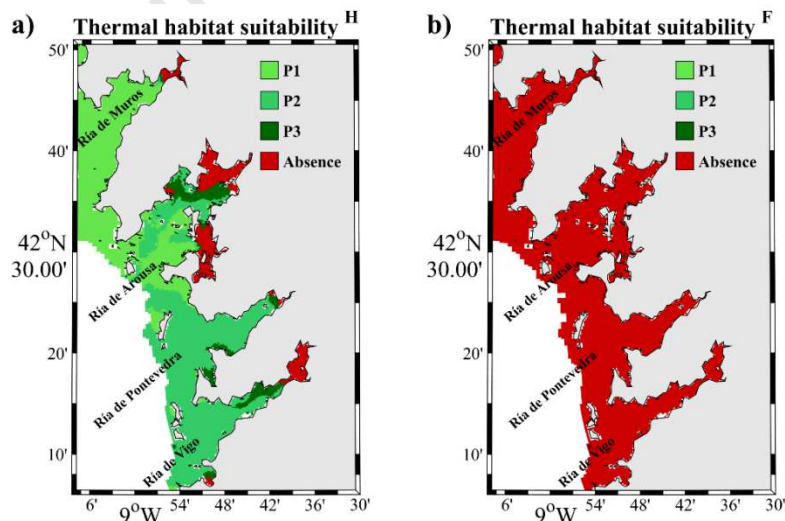
315 3.3. Maps of thermal habitat suitability

316 The potential effect of SST warming on the geographical distribution of *H.*
317 *elongata* and *B. bifurcata* was estimated comparing the geographical map of thermal
318 habitat suitability for the far future (2080-2099) with the present map (1999-2018).

319 The map of thermal habitat suitability of *H. elongata* for the present (Fig. 4a)
320 shows that the thermal conditions of the Rías Baixas are mostly favorable to the
321 presence of the alga. The inner part of the rias, part from the existence of muddy
322 bottoms and low wave agitation, shows unfavorable thermal conditions since upwelling,
323 which reduces water temperature, is negligible. A more detailed analysis shows that the
324 rias of Muros and Arousa display the most suitable conditions, although the time under
325 lethal conditions increases in the middle part of the Ría de Arousa compared with the
326 outer part. The rias of Pontevedra and Vigo show thermal conditions in the P2 range,
327 indicating that the thermal conditions of these two rias are slightly less favorable than
328 those in the other two northern rias. The records of presence/absence of *H. elongata* and
329 other species of cold-temperate intertidal fucaceae, e.g., *Fucus serratus* (L.), collected
330 during a field survey by Martínez et al. (2012), show a higher presence in the rias of
331 Muros and Arousa than in the rias of Pontevedra and Vigo. These observations support
332 the differences in thermal conditions between the Rías Baixas, since a greater presence
333 was recorded in the rias where thermal conditions are more favorable.

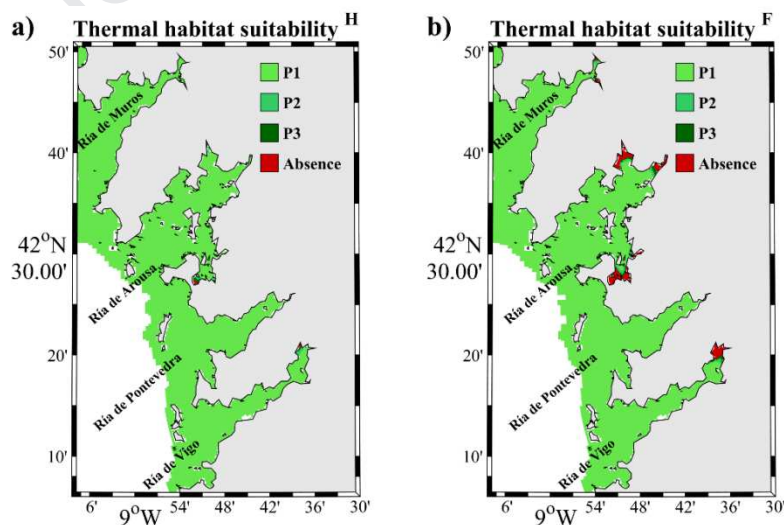
334 Projections for the far future (Fig. 4b) under the RCP 8.5 greenhouse gas
335 emission scenario indicate that thermal conditions in the Rías Baixas will be lethal for
336 *H. elongata*, which implies that this species is projected to disappear. A range
337 contraction of 21% was already estimated for this species by the reduction in its extent
338 of occurrence in the Cantabrian Sea and Portuguese coast between the periods 1980's-
339 1990's to 2013-2016, as part of a general declining trend observed for many cold-
340 temperate fucoids and kelps at its southern range limit in the Iberian Peninsula (Duarte

341 et al., 2013; Casado-Amezúa et al., 2019). *Himanthalia elongata*, together with other
 342 species, was suggested to be included in the red list of endangered species of the
 343 Spanish government, a decision supported by the results of this study. Currently, the
 344 signs of decline inside the rias are less than elsewhere in the open shore, so it can be
 345 considered that they are acting as contemporary refugia to warming for several species
 346 (Duarte and Viejo, 2018). In the same way, an important habitat-forming species, the
 347 kelp *Laminaria hyperborea* (Gunnerus) Foslie, with an upper lethal threshold of 23 °C,
 348 has also suffered a decline inside the Galician rias (Casado-Amezúa et al., 2019). The
 349 decline of temperate macroalgae does not occur locally or regionally, it is becoming
 350 evident as global warming proceeds in areas as far as Australia and South Africa
 351 (Wernberg et al., 2016, 2013; IPCC, 2019). Therefore, in the case of *H. elongata*, whose
 352 tolerance limit (18 °C) is lower than that of *L. hyperborea* (23 °C), it can be considered
 353 that, the Rías Baixas will no longer be refugia for this species by the end of the century
 354 under a RCP8.5 greenhouse gas emission scenario.



355
 356 **Fig. 4.** Thermal habitat suitability for *H. elongata* based on modeled SST for July-August
 357 for the present (1999- 2018) (a) and the far future (2080-2099) (b). Green scale represents areas
 358 suitable for presence and red for absence. P1 represents optimal conditions, P2 intermediate
 359 conditions and P3 sub-lethal SST conditions.

360 Regarding *B. bifurcata*, whose lethal temperature threshold is higher
 361 (24.7°C) than *H. elongata* (18 °C), results for the present (Fig. 5a) show that the
 362 thermal conditions of the Rías Baixas are favorable to the presence of the alga. By
 363 the end of the century (Fig. 5b), this situation may not vary greatly, and only the
 364 innermost part of the rias may turn inappropriate for the algae. As previously stated,
 365 the rias are considered contemporary refugia against seawater warming for several
 366 species (Duarte and Viejo, 2018) because their tendency towards warming is lower
 367 than the trend of adjacent coastal areas. This lower tendency is due to the fact that
 368 the rias are located in the northern limit of the eastern North Atlantic Upwelling
 369 system which buffers the ocean warming (Santos et al., 2011, 2012ab; Bakun et al.,
 370 2015; Varela et al., 2018; Seabra et al., 2019). Thereby, and although the upwelling
 371 may be less effective in the future (Sousa et al. 2020), the water temperature within
 372 the rias will continue to be lower than at the adjacent coastal areas and, then, they
 373 potentially represent climatic refugia for the persistence of *B. bifurcata*, and other
 374 species of similar thermal tolerance.

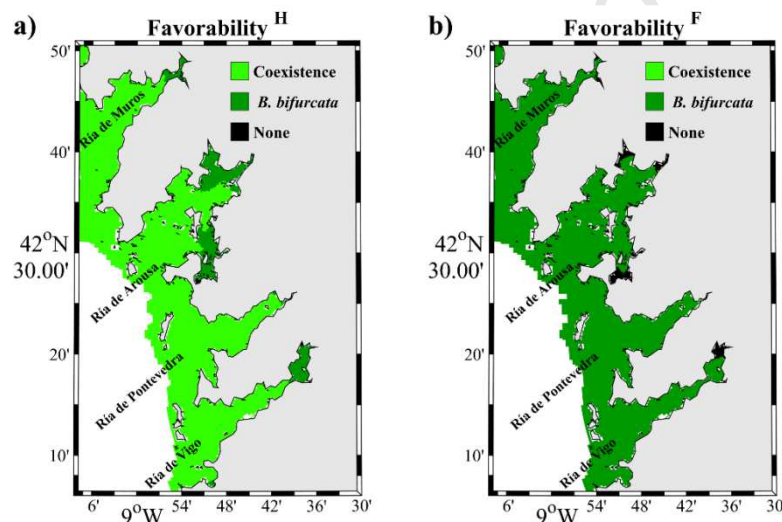


375
 376 **Fig. 5.** Thermal habitat suitability for *B. bifurcata* based on modeled SST for July-August for the
 377 present (1999- 2018) (a) and the far future (2080-2099) (b). Green scale represents areas suitable for

378 presence and red for absence. P1 represents optimal conditions, P2 intermediate conditions and P3 sub-
379 optimal and sub-lethal SST conditions.

380 The upper survival thresholds of other habitat-forming macroalgae are similar to
381 that of *B. bifurcata*. Large intertidal fucoids, namely *Fucus serratus* (L.) and
382 *Ascophyllum nodosum* (L.) Le Jolis, have shown lethal conditions for seawater
383 temperature at about 24 and 25 °C, respectively. In addition, these species are also
384 influenced by stress during emersion that may act in synergy with seawater warming.
385 The threatened kelp *Laminaria ochroleuca* (Bachelot de la Pylaie, 1824), which is a
386 foundational species known to support kelp forests in the NW Iberian Peninsula
387 (Voerman et al., 2013), has been shown to die back at 24.6 °C (Franco et al., 2018). The
388 abundant annual kelp *Saccorhiza polyschides* (Lightfoot) Batters, has an upper survival
389 threshold of 24-25°C (tom Dieck and de Oliveira, 1993). Arrotes (2002) reported an
390 expansion of *F. serratus* and a contraction of *B. bifurcata* in northern Spain in the 90's,
391 this contrasting pattern was associated with a competitive displacement of the resident
392 species (*B. bifurcata*) by the invasive species (*F. serratus*). Currently, the distribution of
393 these species is suffering a drastic contraction in their extent of occurrence in the
394 Cantabrian Sea and Portuguese coast, as well as local declines in abundance in some
395 populations inside the rias, but most populations currently have found refugia inside the
396 rias (Casado-Amezúa et al., 2019). Thus, we may hypothesize that the water thermal
397 conditions of the Rías Baixas will be favorable for all these species, as exemplified in
398 this study by *B. bifurcata*. Once the thermal conditions are suitable, the distribution of
399 the macroalgae species communities will be linked to other environmental factors, such
400 as substrate, air temperature and significant wave height (Martínez et al., 2012, De la
401 Hoz et al., 2019; Ramos et al., 2020). Moreover, the distribution of the macroalgae will
402 also depend on their dispersal ability.

403 Favorability maps (Fig. 6) also confirm that by the end of the century (Fig. 6b)
 404 the increase in the water temperature of the rias may lead to increased prevalence of *B.*
 405 *bifurcata* or the aforementioned habitat-forming species of similar thermal tolerance
 406 such as *Saccorhiza*. Our findings are in accordance with observations by Ramos et al.
 407 (2020), who have recorded an increase of *B. bifurcata*, *Cystoseira baccata*
 408 (S.G.Gmelin) P.C.Silva, *Caulacanthus ustulatus* (Mert. ex Turner) Kütz. and
 409 *Chondracanthus acicularis* (Roth) Fredericq in the Rías Baixas and the decrease of *H.*
 410 *elongata* in Northern Spain.



411
 412 **Fig. 6.** Favorability maps for *H. elongata* and *B. bifurcata* based on lethal conditions for
 413 July-August for the present (1999- 2018) (a) and the far future (2080- 2099) (b). Light green
 414 represents the coexistence of both species, dark green the prevalence of *B. bifurcata* and black the
 415 absence of both species.

416 4. Conclusions.

417 The mechanistic distribution model developed, based on the thermal survival
 418 threshold, projects a shift in the macroalgae species communities by the end of the
 419 century.

420 Ocean warming will increase the exposure time of macroalgae to heatwaves, this
421 increase can lead to the local extinction of *H. elongata* and other macroalgae with a
422 similar thermal tolerance.

423 The analysis of the suitability of the thermal habitat for *B. bifurcata*, whose
424 thermal survival threshold is higher than that of *H. elongata*, shows that thermal
425 conditions by the end of the century can favor the settlement of these macroalgae and
426 other habitat-forming species with a similar thermal tolerance, which makes the Rias
427 Baixas remain as refugia for these species.

428 Although changes in macroalgal species communities will be led by ocean
429 warming, other environmental parameters should be studied. A downscaling of air
430 temperature projections and numerical simulations of wave height inside the rias could
431 contribute to project shifts in the macroalgae species communities more accurately.
432 Furthermore, the developed model can be used to evaluate possible changes in
433 distribution when evaluating different climate change scenarios, as well as for the near
434 future.

435 **Acknowledgements**

436 The authors thank the *Confederación Hidrográfica Miño-Sil*, *MeteoGalicia* and
437 the Hype Web portal for the distribution of river discharge data, the Copernicus Marine
438 Service website for the distribution of IBI data, the General Fishing Secretary, the
439 Spanish Navy Hydrographical Institute and General Bathymetry Chart of the Oceans for
440 the bathymetry data, the WCRP's Working Group on Regional Climate, and the
441 Working Group on Coupled Modelling, former coordinating body of CORDEX and
442 responsible panel for CMIP5. We also thank the climate modelling groups for
443 producing and making available their models' outputs that can be downloaded at
444 <http://www.cordex.org/>.

445 M.D. was supported by the Xunta de Galicia through a doctoral grant (ED481A-
446 2016/218). MCS was supported by national funds (OE), through FCT, I.P., in the scope
447 of the framework contract foreseen in the numbers 4, 5 and 6 of the article 23, of the
448 Decree-Law 57/2016, of August 29, changed by Law 57/2017, of July 19.

449 This work was partially financed by Xunta de Galicia (Spain) under project
450 ED431C 2017/64 "Programa de Consolidación e Estructuración
451 de Unidades de Investigación Competitivas". This work was also funded by European
452 Regional Development Fund under Interreg project "MarRISK"
453 (0262_MARRISK_1_E).

454

455 **References**

456 Anadón, R., 1983. Zonación en la costa asturiana: variación longitudinal de las
457 comunidades de macrófitos en diferentes niveles de marea. *Investigación*
458 *Pesquera* 47, 125–141.

459 Arrontes, J., 2002. Mechanisms of range expansion in the intertidal brown alga
460 *Fucusserratus* in northern Spain. *Marine Biology* 141, 1059–1067.

461 Ashcroft, M.B., 2010. Identifying refugia from climate change: Identifying refugia from
462 climate change. *J. Biogeogr.* 37, 1407-1413. [https://doi.org/10.1111/j.1365-](https://doi.org/10.1111/j.1365-2699.2010.02300.x)
463 [2699.2010.02300.x](https://doi.org/10.1111/j.1365-2699.2010.02300.x)

464 Bakun, A., 1990. Global climate change and intensification of coastal ocean upwelling.
465 *Science* 247, 198–201.

466 Bakun, A., Black, B.A., Bograd, S.J., García-Reyes, M., Miller, A.J., Rykaczewski,
467 R.R., Sydeman, W.J., 2015. Anticipated Effects of Climate Change on Coastal
468 Upwelling Ecosystems. *Curr. Clim. Change Rep.* 1, 85–93.
469 <https://doi.org/10.1007/s40641-015-0008-4>

- 470 Brown, P.T., Caldeira, K., 2017. Greater future global warming inferred from Earth's
471 recent energy budget. *Nature* 552, 45–50. <https://doi.org/10.1038/nature24672>
- 472 Cane, M.A., Clement, A.C., Kaplan, A., Kushnir, Y., Pozdnyakov, D., Seager, R.,
473 Zebiak, S.E., Murtugudde, R., 1997. Twentieth-Century Sea Surface
474 Temperature Trends. *Science* 275, 957–960.
475 <https://doi.org/10.1126/science.275.5302.957>
- 476 Casado-Amezúa, P., Araújo, R., Bárbara, I., Bermejo, R., Borja, Á., Díez, I., Fernández,
477 C., Gorostiaga, J.M., Guinda, X., Hernández, I., Juanes, J.A., Peña, V., Peteiro,
478 C., Puente, A., Quintana, I., Tuya, F., Viejo, R.M., Altamirano, M., Gallardo, T.,
479 Martínez, B., 2019. Distributional shifts of canopy-forming seaweeds from the
480 Atlantic coast of Southern Europe. *Biodivers. Conserv.* 28, 1151–1172.
481 <https://doi.org/10.1007/s10531-019-01716-9>
- 482 Chen, I.-C., Hill, J.K., Ohlemuller, R., Roy, D.B., Thomas, C.D., 2011. Rapid Range
483 Shifts of Species Associated with High Levels of Climate Warming. *Science*
484 333, 1024–1026. <https://doi.org/10.1126/science.1206432>
- 485 Costoya, X., Fernández-Nóvoa, D., deCastro, M., Gómez-Gesteira, M., 2017. Loire and
486 Gironde turbid plumes: Characterization and influence on thermohaline
487 properties. *J. Sea Res.* 130, 7–16. <https://doi.org/10.1016/j.seares.2017.04.003>
- 488 Costoya, X., Fernández-Nóvoa, D., deCastro, M., Santos, F., Lazure, P., Gómez-
489 Gesteira, M., 2016. Modulation of sea surface temperature warming in the Bay
490 of Biscay by Loire and Gironde Rivers. *J. Geophys. Res. Oceans* 121, 966–979.
491 <https://doi.org/10.1002/2015JC011157>
- 492 de la Hoz, C.F., Ramos, E., Puente, A., Juanes, J.A., 2019. Temporal transferability of
493 marine distribution models: The role of algorithm selection. *Ecological*
494 *Indicators* 106, 105499.

- 495 de Pablo, H., Sobrinho, J., Garcia, M., Campuzano, F., Juliano, M., Neves, R., 2019.
496 Validation of the 3D-MOHID Hydrodynamic Model for the Tagus Coastal Area.
497 Water 11, 1713.
- 498 Des, M., deCastro, M., Sousa, M.C., Dias, J.M., Gómez-Gesteira, M., 2019.
499 Hydrodynamics of river plume intrusion into an adjacent estuary: The Minho
500 River and Ria de Vigo. J. Mar. Syst. 189, 87–97.
501 <https://doi.org/10.1016/j.jmarsys.2018.10.003>
- 502 Des, M., Gómez-Gesteira, M., deCastro, M., Gómez-Gesteira, L., Sousa, M.C., 2020.
503 How can ocean warming at the NW Iberian Peninsula affect mussel
504 aquaculture? Sci. Total Environ. 709, 136117.
505 <https://doi.org/10.1016/j.scitotenv.2019.136117>
- 506 Díez, I., Muguerra, N., Santolaria, A., Ganzedo, U., Gorostiaga, J.M., 2012. Seaweed
507 assemblage changes in the eastern Cantabrian Sea and their potential
508 relationship to climate change. Estuarine, coastal and shelf science 99, 108–120.
- 509 Díez, I., Santolaria, A., Secilla, A., Gorostiaga, J.M., 2009. Recovery stages over long-
510 term monitoring of the intertidal vegetation in the ‘Abra de Bilbao’ area and on
511 the adjacent coast (N. Spain). European Journal of Phycology 44, 1–14.
- 512 Duarte, L., Viejo, R.M., 2018. Environmental and phenotypic heterogeneity of
513 populations at the trailing range-edge of the habitat-forming macroalga *Fucus*
514 *serratus*. Mar. Environ. Res. 136, 16–26.
515 <https://doi.org/10.1016/j.marenvres.2018.02.004>
- 516 Duarte, L., Viejo, R.M., Martínez, B., deCastro, M., Gómez-Gesteira, M., Gallardo, T.,
517 2013. Recent and historical range shifts of two canopy-forming seaweeds in
518 North Spain and the link with trends in sea surface temperature. Acta
519 Oecologica 51, 1–10. <https://doi.org/10.1016/j.actao.2013.05.002>

- 520 Evans, G., Prego, R., 2003. Rias, estuaries and incised valleys: is a ria an estuary? *Mar.*
521 *Geol.* 196, 171–175. [https://doi.org/10.1016/S0025-3227\(03\)00048-3](https://doi.org/10.1016/S0025-3227(03)00048-3)
- 522 Fairweather, P.G., 1990. Sewage and the biota on seashores: assessment of impact in
523 relation to natural variability. *Environmental Monitoring and Assessment* 14,
524 197–210.
- 525 Fernández, C., Niell, F.X., Anadón, R., 1983. Comparación de dos comunidades de
526 horizontes intermareales con abundancia de *Bifurcaria bifurcata* Ros. en las
527 costas N y NO de España. *Investigación Pesquera* 47, 435–455.
- 528 Franco, J.N., Tuya, F., Bertocci, I., Rodríguez, L., Martínez, B., Sousa-Pinto, I., Arenas,
529 F., 2018. The ‘golden kelp’ *Laminaria ochroleuca* under global change:
530 Integrating multiple eco-physiological responses with species distribution
531 models. *J. Ecol.* 106, 47–58. <https://doi.org/10.1111/1365-2745.12810>
- 532 Gestoso, I., Olabarria, C., Troncoso, J.S., 2010. Variability of epifaunal assemblages
533 associated with native and invasive macroalgae. *Marine and freshwater research*
534 61, 724–731.
- 535 Hawkins, S.L., Hartnoll, R.G., 1985. Factors determining the upper limits of intertidal
536 canopy-forming algae. *Marine Ecology-Progress Series* 20, 265-271.1985.
- 537 Helmuth, B., Broitman, B.R., Blanchette, C.A., Gilman, S., Halpin, P., Harley, C.D.G.,
538 O’Donnell, M.J., Hofmann, G.E., Menge, B., Strickland, D., 2006. Mosaic
539 patterns of thermal stress in the rocky intertidal zone: implications for climate
540 change. *Ecol. Monogr.* 76, 461–479. [https://doi.org/10.1890/0012-](https://doi.org/10.1890/0012-9615(2006)076[0461:MPOTSI]2.0.CO;2)
541 [9615\(2006\)076\[0461:MPOTSI\]2.0.CO;2](https://doi.org/10.1890/0012-9615(2006)076[0461:MPOTSI]2.0.CO;2)
- 542 IPCC, 2014. *Climate Change 2014: Synthesis Report. Contribution of Working Groups*
543 *I, II and III to the Fifth Assessment Report of the Intergovernmental Panel on*

- 544 Climate Change [Core Writing Team, R.K. Pachauri and L.A. Meyer (eds.)].
545 IPCC, Geneva, Switzerland, 151 pp.
- 546 IPCC, 2019. Bindoff, N.L., W.W.L. Cheung, J.G. Kairo, J. Arístegui, V.A. Guinder, R.
547 Hallberg, N. Hilmi, N. Jiao, M.S. Karim, L. Levin, S. O'Donoghue, S.R. Purca
548 Cuicapusa, B. Rinkevich, T. Suga, A. Tagliabue, and P. Williamson, 2019:
549 Changing Ocean, Marine Ecosystems, and Dependent Communities. In: IPCC
550 Special Report on the Ocean and Cryosphere in a Changing Climate [H.-O.
551 Pörtner, D.C. Roberts, V. Masson-Delmotte, P. Zhai, M. Tignor, E.
552 Poloczanska, K. Mintenbeck, A. Alegría, M. Nicolai, A. Okem, J. Petzold, B.
553 Rama, N.M. Weyer (eds.)]
- 554 Jones, C.G., Lawton, J.H., Shachak, M., 1994. Organisms as Ecosystem Engineers.
555 *Oikos* 69, 373. <https://doi.org/10.2307/3545850>
- 556 Keppel, G., Van Niel, K.P., Wardell-Johnson, G.W., Yates, C.J., Byrne, M., Mucina, L.,
557 Schut, A.G.T., Hopper, S.D., Franklin, S.E., 2012. Refugia: identifying and
558 understanding safe havens for biodiversity under climate change: Identifying
559 and understanding refugia. *Glob. Ecol. Biogeogr.* 21, 393–404.
560 <https://doi.org/10.1111/j.1466-8238.2011.00686.x>
- 561 Krumhansl, K.A., Okamoto, D.K., Rassweiler, A., Novak, M., Bolton, J.J., Cavanaugh,
562 K.C., Connell, S.D., Johnson, C.R., Konar, B., Ling, S.D., 2016. Global patterns
563 of kelp forest change over the past half-century. *Proceedings of the National*
564 *Academy of Sciences* 113, 13785–13790.
- 565 Kumagai, N.H., García Molinos, J., Yamano, H., Takao, S., Fujii, M., Yamanaka, Y.,
566 2018. Ocean currents and herbivory drive macroalgae-to-coral community shift
567 under climate warming. *Proc. Natl. Acad. Sci.* 115, 8990–8995.
568 <https://doi.org/10.1073/pnas.1716826115>

- 569 Lourenço, C.R., Zardi, G.I., McQuaid, C.D., Serrão, E.A., Pearson, G.A., Jacinto, R.,
570 Nicastro, K.R., 2016. Upwelling areas as climate change refugia for the
571 distribution and genetic diversity of a marine macroalga. *J. Biogeogr.* 43, 1595–
572 1607. <https://doi.org/10.1111/jbi.12744>
- 573 Lima, F.P., Ribeiro, P.A., Queiroz, N., Hawkins, S.J., Santos, A.M., 2007. Do
574 distributional shifts of northern and southern species of algae match the warming
575 pattern? *Global change biology* 13, 2592–2604.
- 576 Lüning, K., 1990. *Seaweeds: their environment, biogeography, and ecophysiology*. John
577 Wiley & Sons.
- 578 Martínez, B., Arenas, F., Trilla, A., Viejo, R.M., Carreño, F., 2015. Combining
579 physiological threshold knowledge to species distribution models is key to
580 improving forecasts of the future niche for macroalgae. *Glob. Change Biol.* 21,
581 1422–1433.
- 582 Martínez, B., Viejo, R.M., Carreño, F., Aranda, S.C., 2012. Habitat distribution models
583 for intertidal seaweeds: responses to climatic and non-climatic drivers:
584 Distribution models for intertidal seaweeds in north-western Iberia. *J. Biogeogr.*
585 39, 1877–1890. <https://doi.org/10.1111/j.1365-2699.2012.02741.x>
- 586 McMenamin, S.K., Hadly, E.A., Wright, C.K., 2008. Climatic change and wetland
587 desiccation cause amphibian decline in Yellowstone National Park. *Proc. Natl.*
588 *Acad. Sci.* 105, 16988–16993. <https://doi.org/10.1073/pnas.0809090105>
- 589 Méndez-Sandín, M., Fernández, C., 2016. Changes in the structure and dynamics of
590 marine assemblages dominated by *Bifurcaria bifurcata* and *Cystoseira* species
591 over three decades (1977–2007). *Estuar. Coast. Shelf Sci.* 175, 46–56.
592 <https://doi.org/10.1016/j.ecss.2016.03.015>

- 593 Neiva, J., Assis, J., Coelho, N.C., Fernandes, F., Pearson, G.A., Serrão, E.A., 2015.
594 Genes left behind: climate change threatens cryptic genetic diversity in the
595 canopy-forming seaweed *Bifurcaria bifurcata*. *PloS one* 10.
- 596 Niell, F.X., 1980. Efectos de la destrucción del estrato de *Himanthalia elongata* en la
597 vegetación cespitosa del sistema intermareal de la Ría de Vigo.
- 598 Parmesan, C., Ryrholm, N., Stefanescu, C., Hill, J.K., Thomas, C.D., Descimon, H.,
599 Huntley, B., Kaila, L., Kullberg, J., Tammaru, T., Tennent, W.J., Thomas, J.A.,
600 Warren, M., 1999. Poleward shifts in geographical ranges of butterfly species
601 associated with regional warming. *Nature* 399, 579–583.
602 <https://doi.org/10.1038/21181>
- 603 Poloczanska, E.S., Brown, C.J., Sydeman, W.J., Kiessling, W., Schoeman, D.S., Moore,
604 P.J., Brander, K., Bruno, J.F., Buckley, L.B., Burrows, M.T., Duarte, C.M.,
605 Halpern, B.S., Holding, J., Kappel, C.V., O'Connor, M.I., Pandolfi, J.M.,
606 Parmesan, C., Schwing, F., Thompson, S.A., Richardson, A.J., 2013. Global
607 imprint of climate change on marine life. *Nat. Clim. Change* 3, 919–925.
608 <https://doi.org/10.1038/nclimate1958>
- 609 Poloczanska, E.S., Burrows, M.T., Brown, C.J., García Molinos, J., Halpern, B.S.,
610 Hoegh-Guldberg, O., Kappel, C.V., Moore, P.J., Richardson, A.J., Schoeman,
611 D.S., Sydeman, W.J., 2016. Responses of Marine Organisms to Climate Change
612 across Oceans. *Front. Mar. Sci.* 3. <https://doi.org/10.3389/fmars.2016.00062>
- 613 Russell, B.D., Connell, S.D., Findlay, H.S., Tait, K., Widdicombe, S., Mieszkowska, N.,
614 2013. Ocean acidification and rising temperatures may increase biofilm primary
615 productivity but decrease grazer consumption. *Philos. Trans. R. Soc. B Biol. Sci.*
616 368, 20120438. <https://doi.org/10.1098/rstb.2012.0438>

- 617 Rykaczewski, R.R., Dunne, J.P., Sydeman, W.J., García-Reyes, M., Black, B.A.,
618 Bograd, S.J., 2015. Poleward displacement of coastal upwelling-favorable winds
619 in the ocean's eastern boundary currents through the 21st century. *Geophys.*
620 *Res. Lett.* 42, 6424–6431. <https://doi.org/10.1002/2015GL064694>
- 621 Sánchez, Í., Fernández, C., Arrontes, J., 2005. Long-term changes in the structure of
622 intertidal assemblages after invasion by *Sargassum muticum* (haeophyta).
623 *Journal of Phycology* 41, 942–949.
- 624 Santos, F., Gomez Gesteira, M., deCastro, M Coastal and oceanic SST variability along
625 the western Iberian Peninsula Continental Shelf Research Volume 31, Issue 19-
626 20, December 2011, Pages 2012-2017
- 627 Santos, F., deCastro, M., Gómez-Gesteira, M., Álvarez, I., 2012a. Differences in coastal
628 and oceanic SST warming rates along the Canary upwelling ecosystem from
629 1982 to 2010. *Cont. Shelf Res.* 47, 1–6.
630 <https://doi.org/10.1016/j.csr.2012.07.023>
- 631 Santos, F., Gomez-Gesteira, M., deCastro, M., Alvarez, I., 2012b Differences in coastal
632 and oceanic SST trends due to the strengthening of coastal upwelling along the
633 Benguela current system. *Cont. Shelf Res.* Volume 34, 15 February 2012, Pages
634 79-86. <https://doi.org/10.1016/j.csr.2011.12.004>
- 635 Seabra, R., Varela, R., Santos, A.M., Gómez-Gesteira, M., Meneghesso, C., Wethey,
636 D.S., Lima, F.P., 2019. Reduced Nearshore Warming Associated With Eastern
637 Boundary Upwelling Systems. *Front. Mar. Sci.* 6, 104.
638 <https://doi.org/10.3389/fmars.2019.00104>
- 639 Smale, D.A., Wernberg, T., 2013. Extreme climatic event drives range contraction of a
640 habitat-forming species. *Proc. R. Soc. B Biol. Sci.* 280, 20122829.
641 <https://doi.org/10.1098/rspb.2012.2829>

- 642 Sousa, M.C., deCastro, M., Alvarez, I., Gomez-Gesteira, M., Dias, J.M., 2017. Why
643 coastal upwelling is expected to increase along the western Iberian Peninsula
644 over the next century? *Sci. Total Environ.* 592, 243–251.
645 <https://doi.org/10.1016/j.scitotenv.2017.03.046>
- 646 Sousa, M.C., Ribeiro, A., Des, M., Gomez-Gesteira, M., deCastro, M., Dias, J.M., 2020.
647 NW Iberian Peninsula coastal upwelling future weakening: Competition
648 between wind intensification and surface heating. *Sci. Total Environ.* 703,
649 134808. <https://doi.org/10.1016/j.scitotenv.2019.134808>
- 650 Strain, E.M.A., Thomson, R.J., Micheli, F., Mancuso, F.P., Airoidi, L., 2014.
651 Identifying the interacting roles of stressors in driving the global loss of canopy-
652 forming to mat-forming algae in marine ecosystems. *Glob. Change Biol.* 20,
653 3300–3312. <https://doi.org/10.1111/gcb.12619>
- 654 Sydeman, W.J., García-Reyes, M., Schoeman, D.S., Rykaczewski, R.R., Thompson,
655 S.A., Black, B.A., Bograd, S.J., 2014. Climate change and wind intensification
656 in coastal upwelling ecosystems. *Science* 345, 77–80.
657 <https://doi.org/10.1126/science.1251635>
- 658 tom Dieck, I., de Oliveira, E.C., 1993. The section *Digitatae* of the genus *Laminaria*
659 (*Phaeophyta*) in the northern and southern Atlantic: crossing experiments and
660 temperature responses. *Mar. Biol.* 115, 151–160.
661 <https://doi.org/10.1007/BF00349397>
- 662 Varela, R., Álvarez, I., Santos, F., deCastro, M., Gómez-Gesteira, M., 2015. Has
663 upwelling strengthened along worldwide coasts over 1982-2010? *Sci. Rep.* 5,
664 10016. <https://doi.org/10.1038/srep10016>

- 665 Varela, R., Lima, F.P., Seabra, R., Meneghesso, C., Gómez-Gesteira, M., 2018. Coastal
666 warming and wind-driven upwelling: A global analysis. *Sci. Total Environ.* 639,
667 1501–1511. <https://doi.org/10.1016/j.scitotenv.2018.05.273>
- 668 Voerman, S.E., Llera, E., Rico, J.M., 2013. Climate driven changes in subtidal kelp
669 forest communities in NW Spain. *Marine environmental research* 90, 119–127.
- 670 Wang, D., Gouhier, T.C., Menge, B.A., Ganguly, A.R., 2015. Intensification and spatial
671 homogenization of coastal upwelling under climate change. *Nature* 518, 390–
672 394. <https://doi.org/10.1038/nature14235>
- 673 Wernberg, T., Bennett, S., Babcock, R.C., de Bettignies, T., Cure, K., Depczynski, M.,
674 Dufois, F., Fromont, J., Fulton, C.J., Hovey, R.K., Harvey, E.S., Holmes, T.H.,
675 Kendrick, G.A., Radford, B., Santana-Garcon, J., Saunders, B.J., Smale, D.A.,
676 Thomsen, M.S., Tuckett, C.A., Tuya, F., Vanderklift, M.A., Wilson, S., 2016.
677 Climate-driven regime shift of a temperate marine ecosystem. *Science* 353, 169–
678 172. <https://doi.org/10.1126/science.aad8745>
- 679 Wernberg, T., Smale, D.A., Tuya, F., Thomsen, M.S., Langlois, T.J., de Bettignies, T.,
680 Bennett, S., Rousseaux, C.S., 2013. An extreme climatic event alters marine
681 ecosystem structure in a global biodiversity hotspot. *Nat. Clim. Change* 3, 78–
682 82. <https://doi.org/10.1038/nclimate1627>
- 683 Wiens, J.J., 2016. Climate-Related Local Extinctions Are Already Widespread among
684 Plant and Animal Species. *PLOS Biol.* 14, e2001104.
685 <https://doi.org/10.1371/journal.pbio.2001104>

Highlights

- Climate change impact on habitat-forming macroalgae using numerical predictions
- Ocean warming will increase the exposure time to heatwaves of macroalgae
- *H. elongata* and similar thermal tolerance macroalgae may become extinct locally
- *B. bifurcata* and similar thermal tolerance macroalgae settlements will be favored
- The Rias Baixas will remain as refugia for many species

Journal Pre-proof

Declaration of interests

The authors declare that they have no known competing financial interests or personal relationships that could have appeared to influence the work reported in this paper.

The authors declare the following financial interests/personal relationships which may be considered as potential competing interests:

Journal Pre-proof